INTERNATIONAL JOURNAL OF CLIMATOLOGY
Int. J. Climatol. **24**: 777–790 (2004)
Published online 13 April 2004 in Wiley InterScience (www.interscience.wiley.com). DOI: 10.1002/joc.1029

SUPERENSEMBLE PREDICTION OF REGIONAL PRECIPITATION OVER KOREA

MAENG-KI KIM,[a] IN-SIK KANG,[b,*] CHUNG-KYU PARK[c] and KYU-MYONG KIM[d]
[a] *Department of Atmospheric Science, Kongju National University, 182 Shinkwan-dong, Gongju, 314-701, South Korea*
[b] *School of Earth and Environmental Sciences, Seoul National University, San 56-1 Shinlim-dong, Kwanak-gu, Seoul, 151-742, South Korea*
[c] *Climate Prediction Division, Climate Bureau, Korea Meteorological Administration, 460-18 Shindaebang-dong, Dongjak-gu, Seoul, 156-720, South Korea*
[d] *Science System and Applications, Inc., Lanham, MD, USA*

Received 6 January 2003
Revised 9 January 2004
Accepted 17 January 2004

ABSTRACT

Seasonal precipitation at the decadal time scale is predicted using the downscaling super ensemble (DSE) method, which is developed by combining the superensemble procedure with a statistical downscaling method in this study. The multi-model data utilized are the long-term integration of six atmosphere–ocean general circulation models (AOGCMs) and the downscaling method is based on the singular value decomposition with the empirical orthogonal function (EOF) truncation to correct the systematic bias in the dynamic models.

Interestingly, even though prediction skill in the training period is increased with increasing number of AOGCMs used, the skill is often decreased in the independent period. It is found that prediction skill in the independent period continues to rise when we use an optimal combination of predictors. The optimum combination used in constructing the superensemble model is the super-3 ensemble, which is a combination of three AOGCMs (CCCma, CSIRO, and NCAR) among the six AOGCMs used in this study. In general, the first four EOFs of sea-level pressure (SLP) in the super-3 ensemble are very similar to those of the observed SLP. The dynamic link between Korean winter precipitation and East Asian monsoon circulation in the super-3 ensemble is similar to that of the observed indicating that the super-3 ensemble realistically simulates the circulations in the East Asian monsoon region. The cross-validation for the prediction of the super-3 ensemble shows that the correlation skill score is about 0.49, which is significant at the 5% level. The results provide hope for regional climate prediction in decadal time-scales using superensemble methods together with statistical downscaling. Copyright © 2004 Royal Meteorological Society.

KEY WORDS: superensemble; downscaling; atmospheric circulation; rainfall; general circulation models; East Asia; decadal time scale; Korea

1. INTRODUCTION

Recently, atmospheric variations on an interdecadal time scale have attracted attention from the meteorological community, mainly because of the global warming trend obscured by the interdecadal variation and its large impacts on agricultural production and hydrological management (Trenberth, 1990; Xu, 1993; Busuioc and von Storch, 1996; Solman and Nunez, 1999). The decadal prediction of temperature and precipitation becomes important for long-term water resource management. In the present study, we attempted decadal prediction by combining longer-term atmosphere–ocean general circulation model (AOGCM) simulations and observed data.

The statistical relationship between the observed station data and the observed atmospheric circulation has been studied, and statistical prediction methods have been developed based on the relationship (von

* Correspondence to: In-Sik Kang, School of Earth and Environmental Sciences, Seoul National University, San 56-1 Shinlim–dong, Kwanak–gu, Seoul, 151-742, Korea; e-mail: kang@climate.snu.ac.kr

Storch *et al*., 1993; Muppy, 2000). These relationships are then applied to the circulation simulated by a general circulation model (GCM) in order to generate predictions of local climate (Karl *et al*., 1990; von Storch *et al*., 1993). Statistical downscaling approaches have subsequently emerged to satisfy the need to interpolate regional-scale atmospheric predictor variables to station-scale meteorological series (Kim *et al*., 1984; Wigley *et al*., 1990; Wilby *et al*., 1998). Fundamental to the approach is the assumption that stable empirical relationships can be established between atmospheric processes occurring at disparate temporal and/or spatial scales (Wilby *et al*., 1998).

A multiple regression technique was used by Wigley *et al*. (1990) to derive regression equations linking large-scale spatial averages of precipitation and surface temperature and other large-scale variables to local precipitation and temperature time series on the west coast of the USA. There are lots of similar studies with regression-based downscaling (Wilby *et al*., 1990; Kilsby *et al*., 1998). Von Storch *et al*. (1993) propose a mixed empirical–dynamic approach to translate the large-scale GCM information into a high-resolution distribution by using canonical correlation analysis (CCA) to develop relationships between large-scale monthly sea-level pressure (SLP) fields and local monthly Iberian winter rainfall. They found that the method was skilful in reproducing the observed Iberian Peninsula precipitation anomalies from SLP fields. Wang *et al*. (1999) predicted US precipitation by using the sea-surface temperature (SST) field obtained from the successful prediction of the 1997–98 El Niño by the National Centers for Environmental Prediction (NCEP) coupled model. The assumption in using a coupled model is that the AOGCM produces atmospheric variation with interannual and interdecadal time scales in spite of systematic error. A major part of this systematic error can be corrected by the statistical relationship, or coupled pattern, between the predicted and observed anomalies (Graham *et al*., 1994). The most commonly used methodologies of the coupled pattern technique are based on singular value decomposition analysis (SVDA) and CCA. Ward and Navarra (1997) applied SVDA to simultaneous fields of GCM-simulated precipitation and observed precipitation to correct the errors in model response to SST forcing. CCA has been widely used for a statistical seasonal prediction system (Barnett and Preisendorfer, 1987; Barnston, 1994). A recent study by Feddersen *et al*. (1999), however, demonstrated that the post-processed results are not sensitive to the choice among the methods based on CCA, SVDA, and empirical orthogonal function (EOF) decompositions. In this study, a downscaling superensemble (DSE) method is developed to correct the systematic large-scale model bias by combining a superensemble with a statistical downscaling method that is based on SVDA with EOF truncation. This study is different to the previous studies of Wang *et al*., (1999) and von Storch *et al*. (1993), in that the prediction is based on a superensemble of the downscaling prediction, which is obtained from large-scale predictors of various AOGCMs.

The paper is divided into sections as follows. In Section 2 the data and methodology used in this study are described. The results on the observed links between local climate and large-scale circulation are given and discussed in Section 3. Then, in Section 4, the superensemble predictions are described. The results are discussed and summarized in Section 5.

2. DATA AND METHODOLOGY

The data used in this study are the monthly precipitation of 12 stations in Korea for 49 years from December 1954 to February 2003 (Figure 1). The observed monthly mean SLP was obtained from NCEP–National Center for Atmospheric Research (NCAR) reanalysis data with a horizontal resolution of $2.5^\circ \times 2.5^\circ$ for 45 years from December 1954 to February 1999. The data for the AOGCMs are the monthly mean SLP over the monsoon region (15 °N–70 °N, 60 °E–150 °W) in East Asia. The data were obtained from the Intergovernmental Panel of Climate Change (IPCC)–Data Distribution Center (DDC) for the same period as the observed precipitation. The AOGCM data used in this study are the multi-century control run of NCAR, Canadian Centre for Climate Modeling and Analysis (CCCma), Commonwealth and Scientific Industrial Research Organization (CSIRO), Center for Climate System Research (CCSR), Hadley Centre for Climate Prediction and Research (HCCPR) and Deutsches Klimarechenzentrum (DKRZ) that have participated in

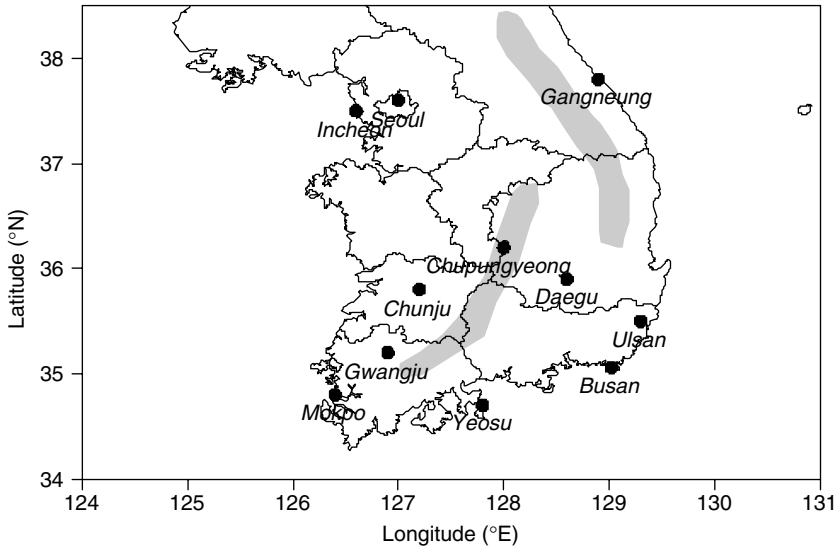

Figure 1. Locations of the 12 Korean stations used in this study. The shaded areas of the Taeback and Soback Mountains are marked in the eastern and the central parts of the Korean peninsula, respectively

Atmospheric model Intercomparison Project–Coupled Model Intercomparison Project. HadCM2 has a spatial resolution of $2.5^\circ \times 3.75^\circ$ and the modelled control climate shows a negligible long-term trend in surface temperature over the first 400 years (Jones *et al*., 1997). CGCM1 of CCCma has a resolution of $3.7^\circ \times 3.75^\circ$ and the control climates of CGCM1 are described by Flato *et al*. (1999). CSIRO-Mk2 has recently been used for a number of more sophisticated climate-change simulations (Hirst *et al*., 2000) and has a spatial resolution of $5.6^\circ \times 3.2^\circ$. The CCSR AOGCM has a spatial resolution of $2.8^\circ \times 2.8^\circ$ and the results of the experiments are discussed by Emori *et al*. (1999). A multi-century control simulation with the coupled model has been performed using the present-day CO_2 concentration (e.g. 345 ppmv in CCSR) to evaluate the stability of the coupled model climate, and to compare the modelled climate and its variability to that observed. Note that the models use flux correction, except for the NCAR AOGCM (Benestad, 2002). Please refer to the IPCC–DDC Webpage for detailed information regarding ECHAM3/LSG and NCAR DOE.

The model bias and error result in low predictability, although this shortcoming can be corrected if the error and bias are systematic (Feddersen *et al*., 1999). The correction procedure, referred to as post-processing, can be developed based on the statistical relationship between the model and the observation. The common methods may be based on SVDA (Feddersen *et al*., 1999) and CCA (von Storch *et al*., 1993) between the observation and the model output. SVDA and CCA are thoroughly described in Bretherton *et al*. (1992). In this study, SVDA with EOF truncation is used to obtain the coupled mode between the large scale and regional scale. Before obtaining the transfer function between the two fields, EOF analysis is applied to the simulated and the observed fields, separately, to reduce the spatial dimensions. After that, SVDA is used to extract coupled modes between the two fields. The covariance matrix in SVDA is constructed by using the normalized time coefficients of EOF analysis in both sides. The downscaling transfer function was constructed as follows:

$$\mathrm{PR}_j(t, x) = \sum_{i=1}^{n} \alpha_i S_i(t) R_i(x) \tag{1}$$

where $\mathrm{PR}_j(t, x)$ indicates the downscaling prediction, $S_i(t)$ is the time coefficient of the SVD mode for the large-scale predictor, and $R_i(x)$ represents the covariance map between regional precipitation and the time coefficients of the SVD mode for the regional-scale predictand. If regional precipitation data are normalized and in addition the expansion coefficients have a variance of one, $R_i(x)$ is identical to the correlation map.

α_i is the correlation coefficient between the time series of the SVD mode of the large-scale predictor and the corresponding SVD time series of the predictand. n is the total number of SVD modes retained.

The superensemble prediction is obtained by weighting the downscaling prediction optimally as follows.

$$P(t) = \beta_0 + \sum_{j=1}^{m} \beta_j \mathrm{PA}_j(\mathrm{t}) \tag{2}$$

where $P(t)$ indicates the superensemble prediction, m is the total number of downscaling predictions, and β indicates the regression coefficients of multiple linear regression analysis. We have used the averaged value $\mathrm{PA}_j(t)$ of station values $\mathrm{PR}_j(t, x)$ obtained from downscaling for simplicity and reduction in error.

3. DOWNSCALING PREDICTION

In this section we discuss the statistical link between observed Korean precipitation and East Asian SLP in the winter season and how much this relationship matches the physical mechanism. The performance of the downscaling model is sensitively dependent on the number of EOFs retained for the SVDA and the number of SVD modes used in the transfer function (Busuioc *et al*., 1999). In order to validate this, the dependence of the skill sensitivity on the number of retained modes is discussed.

The first two EOF modes of winter precipitation are shown in Figure 2. The first EOF mode explains 77.6% of the total variance and has the same sign and magnitude over the entire area, implying that the climate of the Korean peninsula is controlled mainly by the same climate regime that could be linked to a common large-scale circulation process. The time coefficient of the first mode shows the dominant decadal variability and strong signal, especially in the recent period since 1975. In fact, the correlation between the time coefficient of the first mode and averaged precipitation in Korea is about 0.99, indicating that the first

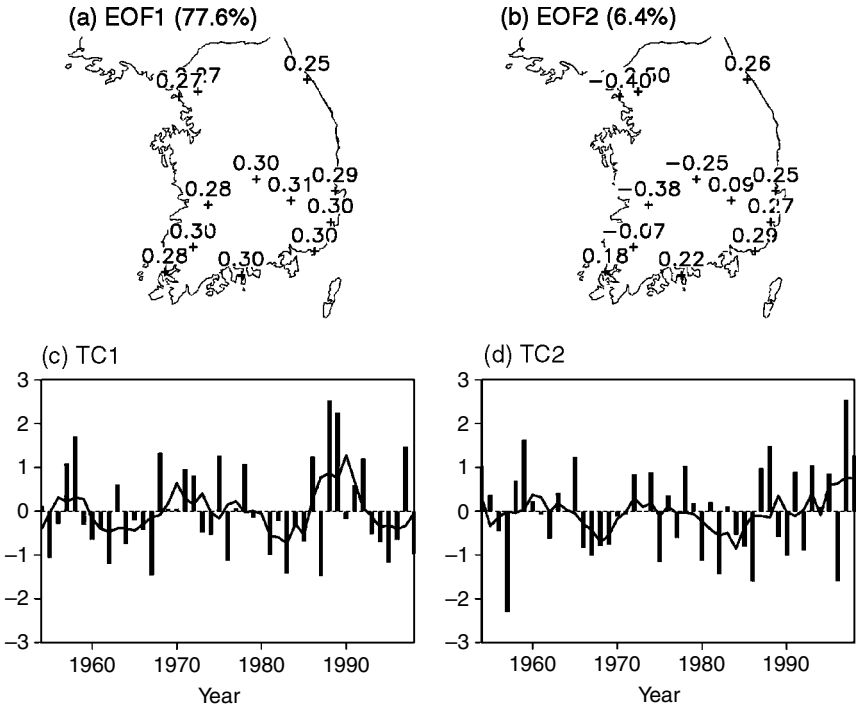

Figure 2. Spatial patterns of (a) the first and (b) the second EOF for winter precipitation in Korea (1954–98). The time coefficients of the first and second modes are shown in (c) and (d) respectively

mode explains much of the variability of Korean precipitation. Compared with the first mode, the second EOF mode (6.4% explained variance) shows the influence of mountains; it has a dipole structure which is separated by two mountains, with one along the east coast and the other along the south coast of the Korean peninsula.

The first two EOFs of SLP show the north–south and east–west patterns in East Asia in the winter season that explain 31.1% and 16.8% of the total variance respectively (Figure 3). The normalized time coefficients of the first two modes are also presented in the lower panel of Figure 3. The first mode shows an increasing trend and the second mode shows decadal variability. In the EOF spatial pattern of the second mode, the Korean peninsula is located in the centre of the dipole structure with one centre of action located over East Asian continent and the other one located in the North Pacific Ocean. This spatial pattern suggests that the warm moist flow from the North Pacific Ocean is enhanced in the positive phase of the time coefficient (i.e. around 1970). The trend mode with the north–south pattern appears to be associated with the warming concentrated at high latitudes, in particular over the continents in the Northern Hemisphere in winter.

Figure 4 shows the first SVD mode between observed SLP and observed precipitation. The correlation coefficient between the expansion coefficients is 0.91 for the first SVD mode, which accounts for 23.2% of total covariance (Figure 4c). Here, the first 10 EOFs of SLP and precipitation have been retained for the subsequent SVDA. The SLP pattern shows an east–west pattern around the Korean peninsula and the precipitation pattern has the same sign over the entire area, although the highest values are in the eastern part and these decrease over the southwestern part. The two spatial patterns of the first SVD mode resemble the EOF patterns shown in Figure 3(b) for large-scale SLP and Figure 2(a) for regional-scale precipitation. These two spatial patterns of the first SVD mode represent a dynamic link that is physically very reasonable, because Korean precipitation is increased (decreased) when anomalous anticyclonic circulation over the North Pacific is intensified (weakened). For example, regional precipitation in the early 1970s is increased by providing the Korean peninsula with warm, moist air by a stronger than normal southeasterly wind. But the pattern is reversed in the early 1980s, mainly due to the strengthening of a cold, dry flow from the continental region.

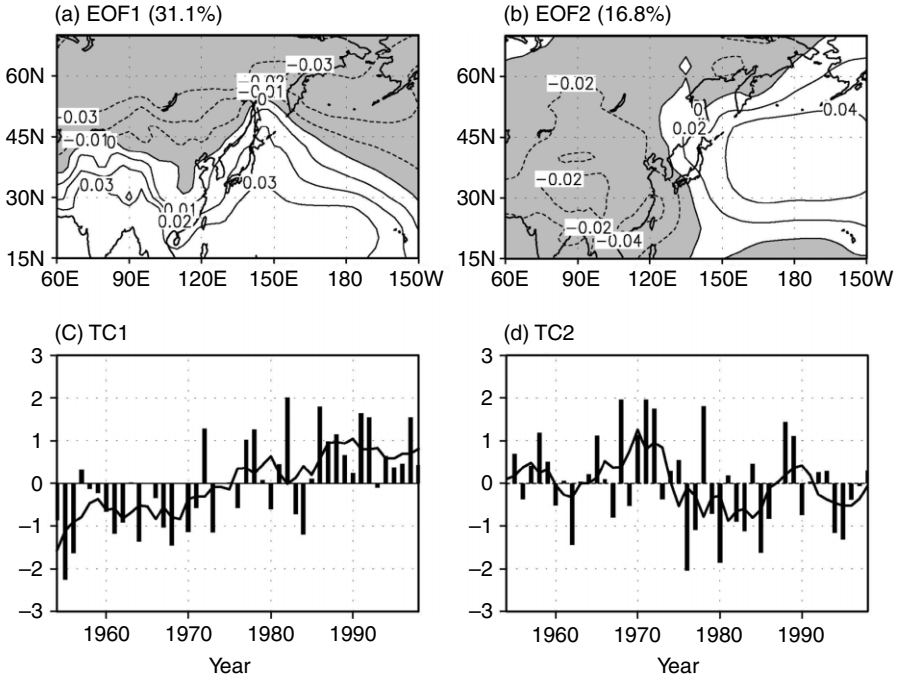

Figure 3. Spatial patterns of (a) the first and (b) the second EOF for the observed winter SLP in East Asia (1954–98). The time coefficients of the first and second modes are shown in (c) and (d) respectively

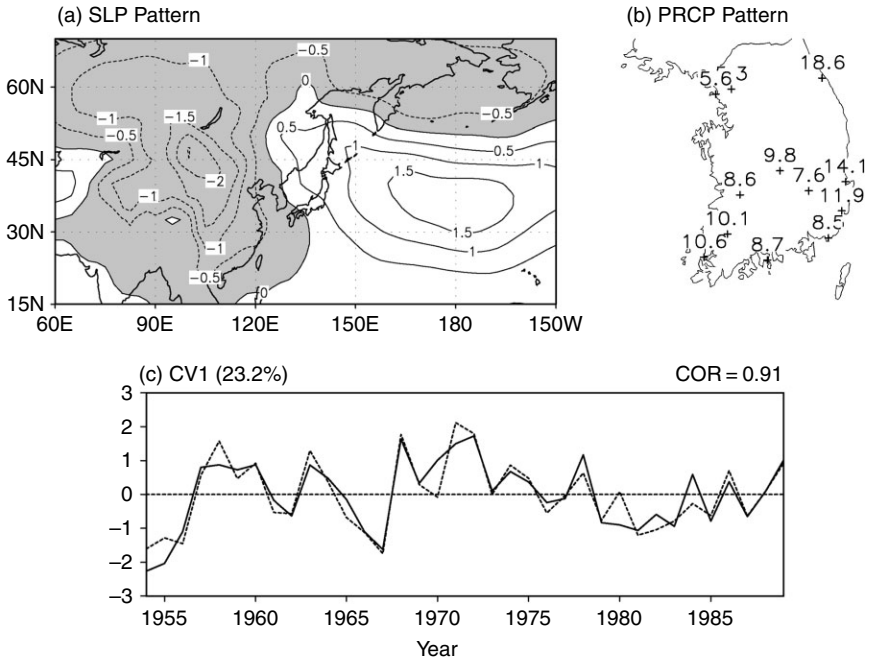

Figure 4. Covariance patterns of (a) the observed SLP in East Asia and (b) winter precipitation of Korea. These patterns explain about 23.2% of total variance. (c) The correlation coefficient (0.91) between the respective amplitude time series of these patterns

The other dipole structure is also located around the North Pacific Ocean with one centre of action at 40 °N latitude and the other centre of weak action around the Bering Sea.

Figure 5(a) and (b) shows the temporal evolution of spatial averages of the estimates obtained from downscaling and of the observed winter precipitation for year-to-year and decadal time scales (5 year running mean) respectively. The correlation coefficient between the observed and the estimated is about 0.79 for the training period and 0.76 in the independent period. The decadal variability shown in Figure 5(b) resembles the time coefficient of the first EOF mode for winter precipitation and of the second EOF mode for the large-scale SLP field, implying that the relationship between the two fields is stable in the coupled mode for the whole period. This suggests that the downscaling technique could be used as an effective tool for downscaling large-scale information simulated by the GCMs or AOGCMs to local scales.

Table I shows the dependence of the skill sensitivity on the number of retained EOF and SVD modes in the observations. Although six modes show better skill than the 10 modes used in this study, which is made subjectively based upon the experience of study, the difference is not large, indicating that correlation skill is not sensitive to the number of retained EOFs in the observations. It is usually emphasized that the length of the verification period is important. But, one needs a reasonably large developmental sample if the resulting equation is to be stable (Wilks, 1995). For example, Busuioc *et al.* (1999) show that the downscaling models are stable using data for 90 years, which satisfies the two conditions of long training and long verification periods. Unfortunately, this is not satisfied in our study. In this study, the decadal mode is important to prediction skill. From lots of tests, we have found that the prediction skill decreased when less than 30 years of data were used in the training period. This is because the coupled mode did not capture the decadal variability in such a short training period. In fact, the variance in the 15 years' time scale is dominant in winter precipitation, which is easily confirmed in Figure 2(c). Therefore, we have concluded that it was better to use at least 30 years, corresponding to two cycles of such a period, in order to pick up this variance in the training period. We have also found that the skill is not sensitive to the number of retained EOFs even in the training period of 30 years, implying that the downscaling models are skilful as long as the decadal mode can be extracted for the training period.

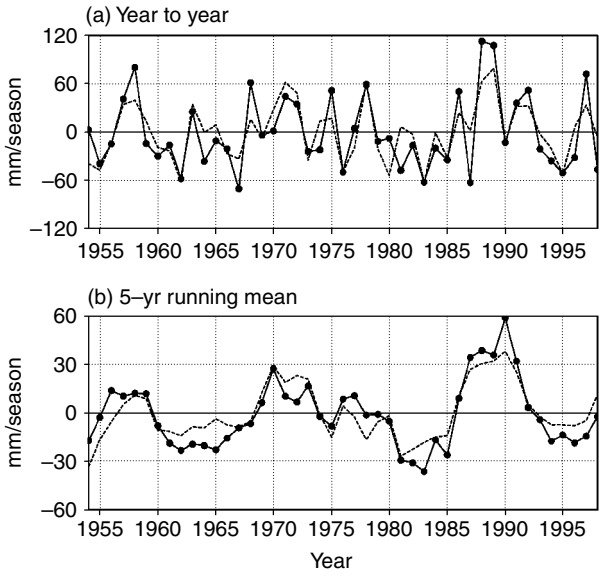

Figure 5. (a) Year-to-year and (b) 5-year running mean time series of the observed (solid line) and the predicted (dashed line) winter precipitation of Korea. The training and verification periods are 36 years (1954–89) and 9 years (1990–98) respectively

Table I. The correlation skill of the statistical downscaling models for various combinations of the number of EOFs of SLP and precipitation (PP) retained for SVDA and the number of SVD pairs used in the statistical downscaling model. The skill is expressed by the correlation coefficients between observed time series and the reconstructed time series obtained from applying the downscaling model to the large-scale observed SLP fields

Number of EOFs		Number of SVDs	Fitting (1954–89)	Verification (1990–98)
SLP	PP			
3	3	3	0.72	0.69
4	4	4	0.74	0.76
5	5	5	0.74	0.76
6	6	6	0.77	0.81
7	7	7	0.78	0.79
8	8	8	0.78	0.78
9	9	9	0.78	0.76
10	10	10	0.79	0.76

4. DOWNSCALING SUPERENSEMBLE PREDICTION

As shown in Section 3, the downscaling model used in this study has reproduced the observed variability of regional precipitation from the large-scale SLP predictor even on a year-to year time scale. This suggests that if the reasonable large-scale predictors of climate models (i.e. AOGCMs) are provided for the statistical downscaling method, the regional climate could be obtained. In this section, we examine the skill of the various AOGCMs, different combinations of AOGCMs, and the sensitivity of the number of retained EOF modes.

Figure 6 shows the temporal evolution of the spatial averages of the estimated and the observed winter precipitation. The estimated precipitation was obtained from the downscaling of the large-scale SLP of the various AOGCMs. The ensemble mean (arithmetic average of predictions) follows the time evolution of the

observed values even though it shows much less variability than the observed precipitation. The downscaling skills of each AOGCM are quite different from each other, even though the estimated precipitation shows a band shape similar to the time evolution. The highest skill appears in the NCAR AOCM, with a correlation of 0.44 for the independent period (1990–2000). CCSR also shows good skill compared with other AOGCMs. This is because the first EOF mode of SLP simulated by the NCAR AOGCM was quite similar to the observed pattern (Figure 3(b)) with the east–west dipole pattern, compared with the other AOGCMs.

Even if all the potential predictors could be assembled and were physically relevant with each other, it would generally not be useful to include all of the potential predictors in the regression analysis. This is because the predictors are almost always mutually correlated, so that the full set of potential predictors contains redundant information (Wilks, 1995). It is well known that the mean-square error on developmental data is underestimated, which is called artificial skill (Glahn, 1985; Michaelson, 1987), implying that the

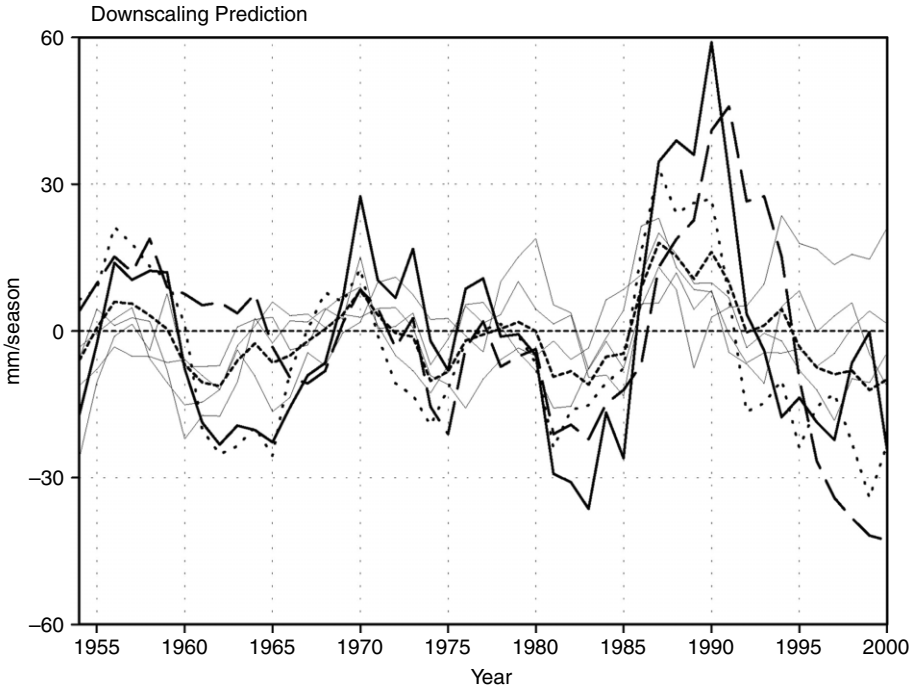

Figure 6. Observed (heavy solid line) and the predicted time series (solid lines) of 5-year running mean winter precipitation of Korea. The downscaling predictions are obtained from Equation (1) by using the SLP predictors of six AOGCMs. The heavy long dashed, dotted and short dashed lines indicate the downscaling prediction by NCAR, CCSR AOGCM predictor and the ensemble mean of six downscaling predictions respectively

Table II. The correlation skill of downscaling superensemble prediction. Super-3 to -6 indicate the optimum superensemble combination based on downscaling prediction obtained from the large-scale predictors of three to six AOGCMs

Case	Training period (1954–89)		Verification period (1990–2000)		AOGCM combination
	Year-to-year	Decadal	Year-to-year	Decadal	
NCAR	0.65	0.61	0.44	0.57	NCAR
Super-3	0.77	0.66	0.77	0.87	NCAR, CCCma, CSIRO
Super-4	0.83	0.77	0.50	0.55	NCAR, CSIRO, CCCma, DKRZ
Super-5	0.87	0.82	0.22	0.45	NCAR, CSIRO, CCCma, DKRZ, CCSR
Super-6	0.89	0.86	0.11	0.36	Six AOGCMs

skill on the developmental data is larger than on independent data. Table II shows the correlation skill of the downscaling superensemble based on Equations (1) and (2). Interestingly, although increasing the number of AOGCMs, that participated in constructing the superensemble model increased the correlation skill in the training period, the correlation skill decreases after arriving at the optimum combination in the independent period. The optimum combination used in constructing the superensemble model is a super-3 ensemble, which is a combination of three of the AOGCMs (CCCma, CSIRO, and NCAR) among the six used in this study. It is well known that the skill in the training period is somewhat proportional to the number of independent variables. But, the prediction skill depends on how much the relationship between the dependent variable and independent variables is physically reasonable and statistically stable over the whole period. Although the skill is perfect in the training period, it is possible to have nearly zero skill in the independent period. This is well known as an overfit regression (Wilks, 1995). Therefore, Table II shows that super-3 ensemble is the most stable, indicating that the regression coefficients are also applicable to the independent period and have not resulted from an overfit regression. We also found that the super-3 ensemble is relatively stable even when using a training period of 30 years. However, it is occasionally unstable for some time spans.

Figure 7(a) and (b) shows the series for the super-3 ensemble prediction (super-3 ensemble in Table II) and the observed precipitation on both interannual and decadal time scales respectively. The time series of the super-3 ensemble prediction in the training period is very similar to that of the observed precipitation, with a correlation coefficient of 0.77, even though it is lower than in the observations shown in Figure 5(a). Even in the independent period there is a high correlation of 0.77, which is significant at the 1% level, even though the independent sample has a small number of degrees of freedom.

Using the mean SLP of the super-3 AOGCMs (CCCma, CSIRO and NCAR), the variability of SLP is analysed in order to verify the performance of the super-3 ensemble. The first two EOFs of the SLP in the super-3 ensemble show east–west and north–south patterns in East Asia in the winter season that explain 23.2% and 15.8% of the total variance respectively (Figure 8(a) and (b)). These patterns resemble the patterns of the observed SLP shown in Figure 3. But, compared with the trend mode of the observed SLP shown in Figure 2(c), the second mode of super-3 shows the decadal mode without the trend, mainly due to the control run data of the AOGCMs (Figure 8(d)). The next two EOFs of SLP in the super-3 ensemble are also very similar to the patterns of the observed SLP (not shown). This suggests that the super-3 ensemble can generate the large-scale patterns corresponding to those of the observations. We conclude that the basic assumption,

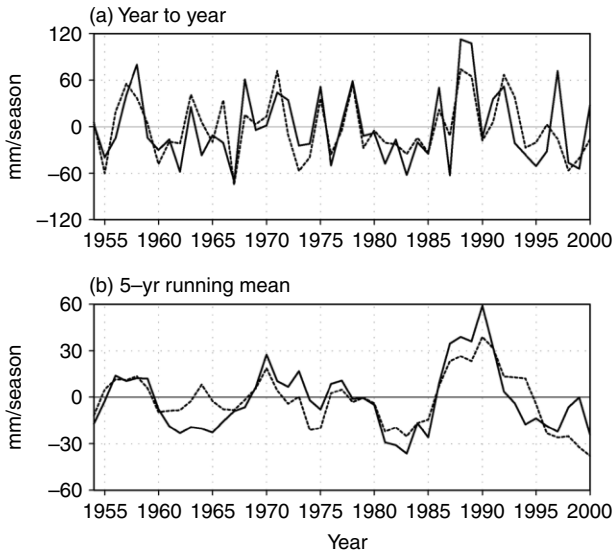

Figure 7. (a) Year-to-year and (b) 5-year running mean time series of the observed (solid line) and the predicted (dashed line) winter precipitation of Korea. The prediction was obtained from Equation (2) with the optimum combination, super-3 ensemble in Table II

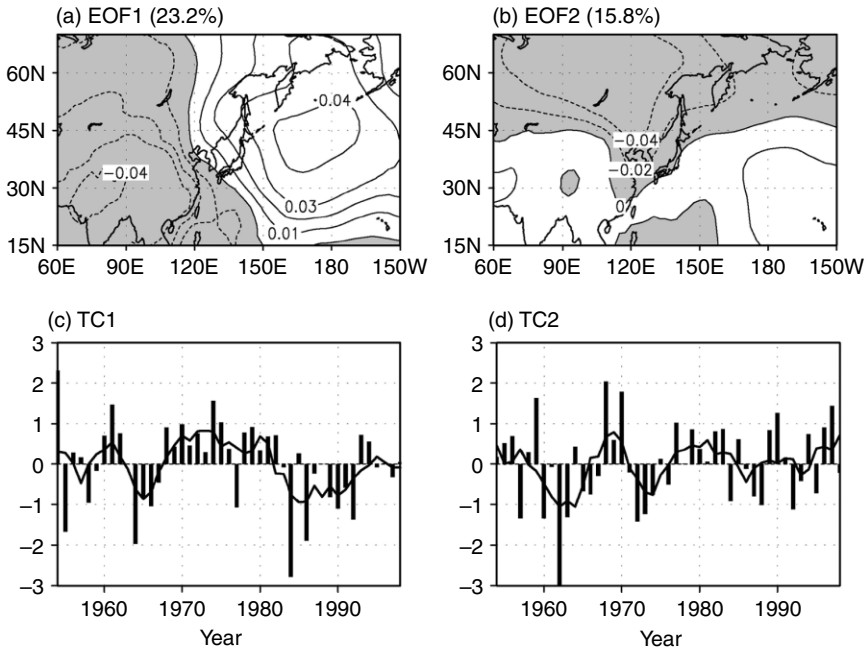

Figure 8. Spatial patterns of (a) the first and (b) the second EOF for winter SLP in East Asia (1954–98) for the super-3 ensemble. The time coefficients of the first and second modes are shown in (c) and (d) respectively

namely that the AOGCMs are doing a credible job on the large scale, is justified, even if the first two model EOFs represent only 39.0% of variance compared with the 47.9% explained by the first two observed EOFs.

The first coupled mode between the SLP of the super-3 ensemble and the observed precipitation (with the largest correlation of 0.7 between the two time coefficients) accounts for 44.7% of the total covariance (Figure 9). The SLP pattern of the super-3 ensemble is similar to the SLP pattern of the observations shown in Figure 4(a), except for the positive signal around the Ural Mountains (Figure 9(a)). The precipitation pattern of the super-3 ensemble has the same sign over the entire area, with the highest values in the eastern part and decreasing over the southwestern part (Figure 9(b)). This pattern is also very similar to the pattern of the observations shown in Figure 4(b). Spatially, these results seem to verify the predictability of the super-3 ensemble. The predictability of the downscaling method depends on the period, the coupled model used, and the target regions. The super ensemble enhances the predictability by using an optimum combination of the prediction of the downscaling method in order to explain the variability of the observed precipitation. In our cases, we did not use the constraint that the sum of weighting is equal to that in multiple regression analysis in order to minimize the error of variance, like Krisnamurti *et al*. (2000). It is noted that this constraint ensures that the prediction is in the range of possible climate (Shen *et al*., 2001). Shen *et al*. (2001) suggested that the results are actually close despite the difference between their method and that of Krisnamurti *et al*. (2000).

In order to verify the predictability of the super-3 ensemble, a cross-validation procedure was applied for the observed period of 49 years from 1954 to 2002. In variant 1, the super-3 ensemble model was constructed by using the data for the 30 years from 1954 to 1983, and then the prediction was obtained in the independent period (1984–2002). In variant 2, the super-3 ensemble model was constructed by using the data for the 30 years from 1973 to 2002, and then the prediction was obtained in the independent period (1954–1972). Table III shows the sensitivity of skill on the number of retained EOF and SVD modes in both variants 1 and 2. Stable and skilful relations appear in retained mode 6 in both variants 1 and 2, even though the relation is weaker than in the observations. The mean correlation skill of the super-3 ensemble for the verification period is about 0.49, which is significant at the 5 % level.

Figure 10 shows the first coupled mode between the super-3 ensemble SLP and observed SLP. The correlation coefficient between the two time coefficients is 0.76. This suggests that the super-3 ensemble

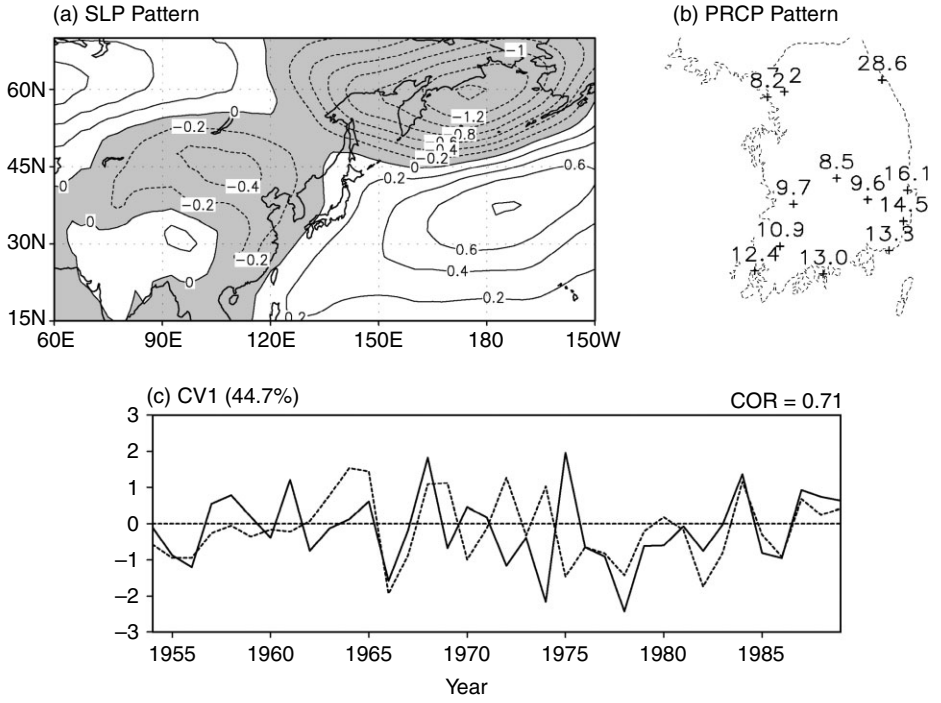

Figure 9. Correlation patterns of (a) the SLP in East Asia for the super-3 ensemble and (b) winter precipitation of Korea. These patterns explain about 44.7% of total variance. (c) The correlation coefficient (0.71) between the respective amplitude time series of these patterns

Table III. The correlation skill (year-to-year/decadal) of the downscaling super-3 ensemble models for various combinations of the number of EOFs of SLP and precipitation (PP) retained for SVDA and the number of SVD pairs used in the statistical downscaling model. The skill is expressed by the correlation coefficients between observed time series and the reconstructed time series obtained from applying the downscaling super-3 ensemble model to the large-scale AOGCM SLP fields

Number of EOFs		Number of SVDs	Variant 1		Variant 2	
SLP	PP		Fitting (1954–83)	Verification (1984–2002)	Fitting (1973–2002)	Verification (1954–72)
3	3	3	0.33/0.52	0.14/−0.23	0.63/0.54	−0.33/−0.19
4	4	4	0.60/0.64	0.25/0.39	0.76/0.84	−0.04/0.30
5	5	5	0.77/0.90	0.31/0.86	0.79/0.85	0.32/0.38
6	6	6	0.83/0.92	0.58/0.85	0.82/0.93	0.41/0.38
7	7	7	0.85/0.88	0.56/0.84	0.89/0.96	0.27/0.10
8	8	8	0.85/0.85	0.60/0.88	0.94/0.97	0.17/0.10
9	9	9	0.85/0.82	0.49/0.82	0.94/0.96	0.16/0.15
10	10	10	0.85/0.87	0.47/0.84	0.93/0.96	0.10/−0.05

reproduces the variability of the observed SLP, especially on the decadal time scale, although there are some discrepancies between the two patterns. This implies that if the decadal variability is generated by ocean variability in the AOGCMs and it is consistent, then coupled modes with observed precipitation are constructed and physically reasonable even though the phase of time evolution of the control run is different from the observations. The pattern of observed SLP shown in Figure 10(a) is similar to the one for precipitation

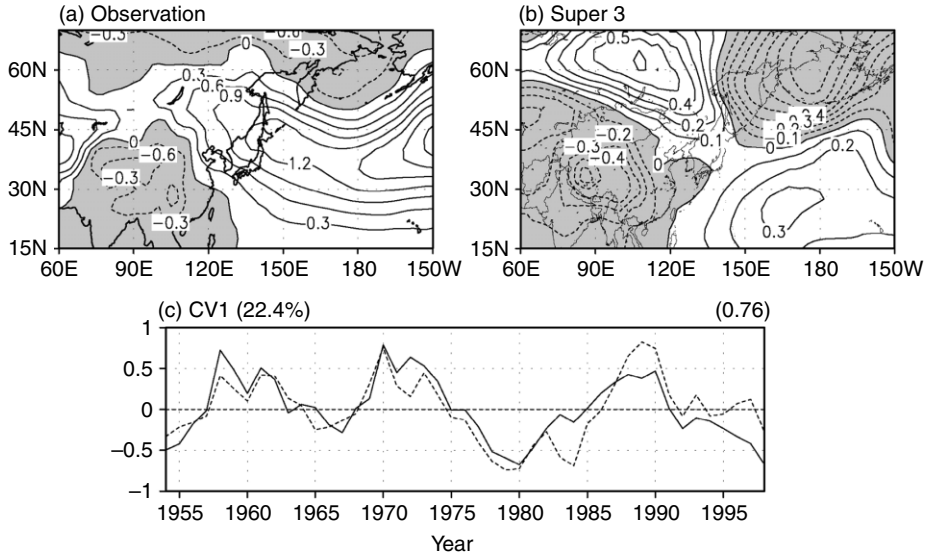

Figure 10. Covariance patterns of the SLP for (a) observation and (b) super-3 ensemble over East Asia. These patterns explain about 22.4% of total variance. (c) The correlation coefficient (0.76) between the respective amplitude time series of these patterns

shown in Figure 4(a). Similarly, the pattern of the super-3 ensemble shown in Figure 10(b) is also similar to the one for precipitation shown in Figure 9(a), although there are some differences.

5. CONCLUSIONS

In this study, some conclusions may be drawn regarding both the methodology and the dynamic link between large scale and regional scale. Some conditions have to be satisfied for the downscaling procedure to be useful (von Storch *et al*., 1993; Busuioc *et al*., 1999). First, the GCMs should be capable of reproducing the large-scale variability realistically. Second, the relationship between the large-scale and regional-scale parameters has to be strong. In this study, it is shown that the superensemble prediction based on the downscaling was satisfied with two conditions, and the dynamics were discussed.

The observed variability of Korean winter precipitation is associated with the second mode of SLP with the east–west dipole pattern. In the EOF spatial pattern of the second mode, the Korean peninsula is located in the centre of the dipole structure with one centre of action located on the East Asian continent and the other one located in the northwest Pacific Ocean. This suggests that the warm moist flow from the northwest Pacific Ocean is enhanced in the positive phase of the time coefficient (i.e. around 1970). The dynamic link between Korean winter precipitation and the East Asian monsoon circulation is very strong, so that the predictability of the downscaling method is very high, even on the year-to-year time scale.

The predictions of Korean winter precipitation were obtained from the superensemble using the downscaling predictions obtained from the SLP predictors of six AOGCMs. Interestingly, although the number of AOGCMs that participated in constructing the superensemble model increased the correlation skill in the training period, the correlation skill decreased after arriving at the optimum combination in the independent period, implying that the relationships between the super-3 ensemble SLP and regional precipitation are physically reasonable and statistically stable over the whole period. The optimum combination used in the super ensemble is the super-3 ensemble, which is a combination of the CCCma, CSIRO, and NCAR AOGCMs. The correlation coefficient between observed and predicted in the super-3 ensemble is about 0.77 for the independent period (1990–2000) on the year-to-year time scale. The performance of the super-3 ensemble is superior to that of the downscaling prediction obtained from the large-scale SLP of any single AOGCM.

Overall, the first four EOFs of SLP in the super-3 ensemble are very similar to those of the observed SLP. The dynamic link between Korean winter precipitation and the East Asian monsoon circulation in the super-3 ensemble is similar to that of the observations, implying that the super-3 ensemble has two conditions to be satisfied for the superensemble procedure to be useful. The predictability of the super-3 ensemble was evaluated by using the cross-validation procedure and the two-tailed t-test. The mean correlation skill of the super-3 ensemble for the verification period is about 0.49, which is significant at the 5 % level.

ACKNOWLEDGEMENT

The present study is supported by a research project of the Ministry of Agriculture and Forestry under project no. 19995043. This study was carried out in the Climate Environmental System Research Center (CES) sponsored by the Korea Science and Engineering Foundation.

REFERENCES

Barnett TP, Preisendorfer R. 1987. Origins and levels of monthly and seasonal forecast skill for United States surface air temperatures determined by canonical correlation analysis. *Monthly Weather Review* **115**: 1825–1850.

Barnston AG. 1994. Linear statistical short-term climate predictive skill in the Northern Hemisphere. *Journal of Climate* **7**: 1513–1564.

Benestad RE. 2002. Empirically downscaled multimodel ensemble temperature and precipitation scenarios for Norway. *Journal of Climate* **15**: 3008–3027.

Brethern CS, Smith C, Wallace JM. 1992. An intercomparison of methods for finding coupled patterns in climate data. *Journal of Climate* **5**: 541–560.

Busuioc A, von Storch H. 1996. Changes in the winter precipitation in Romanis and its relation to the large-scale circulation. *Tellus Series A: Dynamic Meteorology and Oceanography* **48**: 538–552.

Emori S, Nozawa T, Abe-Ouchi A, Numaguti A, Kimoto M, Nakagima T. 1999. Coupled ocean–atmosphere model experiments of future climate change with an explicit representation of sulfate aerosol scattering. *Journal of the Meteorological Society of Japan* **77**: 1299–1307.

Feddersen H, Navarra A, Ward MN. 1999. Reduction of model systematic error by statistical correction for dynamic seasonal prediction. *Journal of Climate* **12**: 1974–1989.

Flato GM, Boer GJ, Lee WG, McFarlane NA, Ramsden D, Reader MC, Weaver AJ. 1999. The Canadian Centre for Climate Modelling and Analysis global coupled model and its climate. *Climate Dynamics* **16**: 451–467.

Glahn HR. 1985. Statistical weather forecasting. In *Probability, Statistics, and Decision Making in the Atmoshperic Sciences* Westview Press: 289–335.

Graham NE, Barnett TP, Wilde R, Ponater M, Schubert S. 1994. On the roles of tropical and midlatitude SSTs in forcing interannual to interdecadal variability in the winter Northern Hemisphere circulation. *Journal of Climate* **7**: 1416–1448.

Hirst AC, O'Farrell SP, Gordon HB. 2000. Comparison of a coupled ocean–atmosphere model with and without oceanic eddy-induced advection. 1. Ocean spin-up and control integrations. *Journal of Climate* **13**: 139–163.

Jones TC, Carnell RE, Crossley JF, Gregory JM, Mitchell JFB, Senior CA, Tett SFB, Wood RA. 1997. The second Hadley Centre coupled ocean–atmosphere GCM: model description, spin-up and validation. *Climate Dynamics* **13**: 103–134.

Karl TR, Wang WC, Schlesinger ME, Knight RW, Portman D. 1990. A method of relating general circulation model simulated climate to the observed local climate. *Journal of Climate* **3**: 1053–1079.

Kilsby CG, Cowpertwait PSP, O'connell PE, Jones PD. 1998. Predicting rainfall statistics in England and Wales using atmospheric circulation variables. *International Journal of Climatology* **18**: 523–539.

Kim JW, Chang JT, Barker NL, Wilks DS, Gates WL. 1984. The statistical problem of climate inversion: determination of the relationship between local and large-scale climate. *Monthly Weather Review* **112**: 2069–2077.

Krisnamurti TN, Kishtawal CM, Shin DW, Willford CE. 2000. Improving tropical precipitation forecasts from a multianalysis superensemble. *Journal of Climate* **13**: 4217–4227.

Michaelson J. 1987. Cross-validation in statistical climate forecast models. *Journal of Climate and Applied Meteorology* **26**: 1589–1600.

Muppy J. 2000. Predictions of climate change over Europe using statistical and dynamical downscaling techniques. *International Journal of Climatology* **20**: 489–501.

Shen SSP, Lau WKM, Kim KM, Li G. 2001. A canonical correlation prediction model for seasonal precipitation anomaly. NASA/TM-2001-209989.

Solman SA, Nunez MN. 1999. Local estimates of global climate change: a statistical downscaling approach. *International Journal of Climatology* **19**: 835–861.

Trenberth KE. 1990. Recent observed interdecadal climate changes in the Northern Hemisphere. *Bulletin of the American Meteorological Society* **71**: 988–993.

Von Storch H, Zorita E, Cubasch E. 1993. Downscaling of global climate estimates to regional scales: an application to the Iberian rainfall in wintertime. *Journal of Climate* **6**: 1161–1171.

Wang H, Ting M, Ji M. 1999. Prediction of seasonal mean United States precipitation based on El Nino sea surface temperatures. *Geophysical Research Letters* **26**: 1341–1344.

Ward MN, Navarra A. 1997. Pattern analysis of SST-forced variability in ensemble GCM simulations: examples over Europe and tropical Pacific. *Journal of Climate* **10**: 2210–2220.

Wigley TML, Jones PD, Briffa KR, Smith G. 1990. Obtaining sub-grid-scale information from coarse-resolution general circulation model output. *Journal of Geophysical Research* **95**(D2): 1943–1953.

Wilby RL, Wigley TML, Conway D, Jones PD, Hewitson BC, Main J, Wilks DS. 1998. Statistical downscaling of general circulation model output: a comparison of methods. *Water Resources Research* **33**(11): 2995–3008.
Wilks DS. 1995. *Statistical Methods in the Atmospheric Sciences*. Academic Press.
Xu JS. 1993. The joint modes of the coupled atmosphere-ocean system observed from 1967 to 1986. *Journal of Climate* **6**: 816–838.

